Residual and Dynamic Range of Retinal Nerve Fiber Layer Thickness in Glaucoma: Comparison of Three OCT Platforms

Jean-Claude Mwanza,[1] Hanna Y. Kim,[2] Donald L. Budenz,[1] Joshua L. Warren,[3] Michael Margolis,[2] Scott D. Lawrence,[1] Pooja D. Jani,[1] Garrett S. Thompson,[1] and Richard K. Lee[2]

[1]Department of Ophthalmology, University of North Carolina, Chapel Hill, North Carolina, United States
[2]Bascom Palmer Eye Institute, Department of Ophthalmology, University of Miami, Miami, Florida, United States
[3]Department of Biostatistics, Yale School of Public Health, Yale University, New Haven, Connecticut, United States

Correspondence: Donald L. Budenz, Bioinformatics Building, CB #7040, Chapel Hill, NC 27599, USA; donald_budenz@med.unc.edu.

Submitted: May 11, 2015
Accepted: August 3, 2015

Citation: Mwanza JC, Kim HY, Budenz DL, et al. Residual and dynamic range of retinal nerve fiber layer thickness in glaucoma: comparison of three OCT platforms. *Invest Ophthalmol Vis Sci*. 2015;56:6344–6351. DOI:10.1167/iovs.15-17248

Purpose. To estimate visual field (VF) sensitivity at which retinal nerve fiber layer (RNFL) thinning reaches the measurement floor and at which RNFL stops thinning (change points), the dynamic range of RNFL thickness, and the number of steps from normal to RNFL floor among three optical coherence tomography (OCT) devices.

Methods. Glaucomatous patients ($n = 58$) and healthy subjects ($n = 55$–60) prospectively underwent VF testing and RNFL thickness measurement with Cirrus, Spectralis, and RTVue. Change points and corresponding RNFL thicknesses were estimated with simple linear regression (SLR) and Bayesian change point (BCP) analyses. The dynamic range and number of steps to RNFL floor were determined.

Results. The average VF change points and corresponding residual thickness at the time RNFL stopped thinning were −22.2 dB and 57.0 μm (Cirrus), −25.3 dB and 49.2 μm (Spectralis), and −24.6 dB and 64.7 μm (RTVue). The RNFL dynamic ranges derived from SLR values were wider on Spectralis (52.6 μm) than on Cirrus (35.4 μm) and RTVue (35.5 μm); the corresponding number of steps to reach the RNFL floor were 9.0 on Cirrus, 10.6 on Spectralis, and 8.3 on RTVue.

Conclusions. The relative VF sensitivity at which average RNFL thickness reaches the measurement floor, the residual layer thickness, and RNFL dynamic measurement range differ among the three devices. However, the number of steps from normal to the RNFL thickness floor is comparable.

Keywords: glaucoma, optical coherence tomography, retinal nerve fiber layer

Assessments of retinal nerve fiber layer (RNFL) and optic nerve head via optical coherence tomography (OCT) and visual field (VF) using standard automated perimetry (SAP) are often used for the diagnosis and management of glaucoma. Performing both tests in patients suspected of having glaucoma or those with definite glaucoma stems from the fact that the disease results in both structural changes affecting inner retinal layers and peripheral VF deficits that may lead to blindness if the disease is left untreated. The assessment of glaucoma-induced structural and functional damage has improved tremendously over the years, which in turn has enhanced the ability to detect and monitor glaucoma. However, this improvement has not translated into a complete understanding of the nature of the relationship between structural damage and functional loss during the course of the disease. Indeed, while it has been established that there is a good relationship between the two components, the natural history of the structure–function relationship in glaucoma has not been completely elucidated. For example, it is still debated whether this relationship is linear or nonlinear.[1–8] Interindividual variability (i.e., some patients show structural changes prior to detectable VF abnormalities while others experience the converse), the difference in structural parameter measurements (i.e., RNFL) obtained with different OCT devices, the type of VF information used (i.e., full sensitivity thresholds, total deviation sensitivities, mean deviation, VF index), and the type of map used for spatial relationship between structural and functional measures are among the factors that may account for discrepancies among studies and the difficulty in better understanding the structure–function relationship in glaucoma. Additional challenges include differences in the dynamic range and the floor of structural measures across devices.

The concept of floor and dynamic range of structural parameters in glaucoma has gained attention recently as a result of improvements in imaging and measuring inner retinal layers and optic nerve head (ONH) structures. Since the first mention of floor of RNFL thickness determined from measurements obtained in glaucomatous eyes with scanning laser polarimetry by Blumenthal et al.,[9] a few other investigators have reported on the same topic using either time-domain OCT[10] or spectral-domain OCT (SDOCT).[11–13] Conceptually, the floor and dynamic range of RNFL thickness are interrelated. Studying both simultaneously may not only improve our understanding of the structure–function relationship but also will provide clinically useful information with regard to glaucoma follow-up. The purpose of the current study was to estimate and compare

the floor and dynamic range of RNFL thickness measured with three different SDOCT devices in patients with glaucoma and to assess the structure–function relationship globally and focally in each case.

Subjects and Methods

Subjects

Following approval of the study protocol by Biomedical Institutional Review Boards of the University of North Carolina at Chapel Hill and the University of Miami, patients 18 years or older with documented moderate to severe primary open-angle glaucoma (POAG) or normal-tension glaucoma (NTG) were consecutively recruited and enrolled in the study in compliance with the tenets of the Declaration of Helsinki. Glaucoma was diagnosed following a complete ophthalmic examination that included fundus ophthalmoscopy, gonioscopy, applanation tonometry, optic disc stereophotography, and VF testing with SAP (24-2 Swedish Interactive Threshold Algorithm program using the Humphrey Visual Field Analyzer [Carl Zeiss Meditec, Inc., Dublin, CA, USA]). Glaucoma was defined based on characteristic glaucomatous ONH damage and typical glaucomatous VF loss (defined as glaucoma hemifield test results outside normal limits, a pattern standard deviation with a P value $< 5\%$, or a cluster of three or more points in the pattern deviation plots in the superior or inferior hemifield with P values $< 5\%$, one of which had to have a $P < 1\%$) in eyes with open iridocorneal angles. Moderate and severe glaucomas were defined using the Hodapp-Anderson-Parrish severity scale.[14] Exclusion criteria for the study were a history of or current retinal disease, nonglaucomatous optic neuropathy, neurologic disease, treatments that may cause optic neuropathy, and a history of intraocular surgery except for glaucoma and cataract surgery performed more than 3 months prior to enrollment.

Data from age-matched normal subjects who participated in the Cirrus HD-OCT (Carl Zeiss Meditec, Inc.) and RTVue (Optovue, Inc., Fremont, CA, USA) were also used. In addition, the Spectralis OCT (Heidelberg Engineering, Heidelberg, Germany) RNFL data of normal subjects used for this analysis were provided by the investigators of the National Eye Institute–sponsored Diagnostic Innovations in Glaucoma Study conducted at the University of California-San Diego, San Diego, California (UCSD). Exclusion criteria for normal subjects included IOP $\geq$ 22 mm Hg or history of elevated IOP; any type of glaucoma in either eye; intraocular surgery in the study eye (except uncomplicated cataract or refractive surgery performed more than 3 months prior to enrolment); best-corrected visual acuity worse than 20/40; evidence of diabetic retinopathy, macular edema, or other vitreoretinal disease; or evidence of optic nerve abnormality in either eye. Subjects with cup-to-disc ratio (CDR) asymmetry $\geq$ 0.2 or an abnormal VF indicated by a pattern standard deviation (PSD) outside 95% confidence limits or a glaucoma hemifield test (GHT) result outside normal limits were also excluded.

RNFL Thickness Measurement

All patients underwent RNFL thickness measurement with Cirrus HD-OCT, Spectralis OCT, and RTVue during the same session. The peripapillary circular sampling pattern (3.4-mm circle centered on the optic disc) was used on each instrument for RNFL thickness measurements. Only high-quality scans defined as those with good quality score (signal strength $\geq$ 6 for Cirrus, quality score $\geq$ 20 for Spectralis, and signal strength index $\geq$ 30 for RTVue) and without segmentation failure and no eye movement or blinking artifacts were retained for analysis. The overall average RNFL and averages of the superior and inferior quadrant RNFL thicknesses were used for analysis in this study.

Visual Field Data Handling

Only reliable VFs ($\leq$33% false positives or false negatives, and $\leq$15% fixation losses) were used in this study. The analyses in this study used all 52 relative sensitivity values (expressed in dB) from the total deviation numerical plot. For spatial correlation between quadrant RNFL and corresponding VF sectors, we used a VF map with four VF sectors (superior and inferior: 21 test data points each) as we recently described,[15] but only the superior and inferior field sectors were considered for analysis. For each field sector, the relative sensitivity was obtained by averaging all the sector's data point relative sensitivities. The averaging was performed after the total deviation values were antilogged as previously described by Hood and Kardon.[6] The global relative sensitivity was the average of all 52 data point sensitivities. Left eye data were converted to right eye format for consistency.

RNFL Residual Estimation

The residual thickness was determined using two methods that estimated the change point, which is the relative retinal sensitivity at which the RNFL stops getting measurably thinner, and the corresponding residual thickness. The first method, a Bayesian change point (BCP) analysis, is derived from the Hood and Kardon model[6] that we modified and fit in the Bayesian setting.[16] The purpose of the modification was to model the data for RNFL thickness to flatten out from a certain value of relative VF sensitivity, so that RNFL measurements will stop getting thinner despite continuous VF loss. Details about this model have been described elsewhere.[15] The second method, a simple linear regression change point (SLRCP) analysis, is a derivation of the tipping point of the relationship between RNFL thickness and visual function described by Wollstein et al.[17] In this method we used simple linear regression lines of the relationship between RNFL thickness and relative VF sensitivity. First, a series of regression line pairs were plotted, one in the steep and another in the plateau portion of the relationship, which allowed for the determination of the location of the change in slope steepness. Finally, the pairs of regression lines were compared in terms of slope, and the pair with the most pronounced slope in the steep portion and the least slope in the plateau portion of the relationship was considered as best fitting the data. Fourth, the intersection between the two regression lines was identified as the change point, which allowed easy determination of its corresponding coordinate on the relative VF sensitivity axis. In both methods (BCP and SLRCP), knowing the change point allowed the determination of post–change point residual layer thickness and its corresponding relative VF sensitivity.

Due to the interindividual variability in residual thickness and change points, we calculated the post–change point residual layer thickness and corresponding relative VF sensitivity by averaging all RNFL thicknesses with VF sensitivity equal to or worse than the change point globally and for each sector. The post–change point residual layer thickness and relative VF sensitivity were considered as the measured residual thickness and relative VF sensitivity, respectively. Student's t-tests were used to compare mean post–change point residual layer thicknesses with corresponding relative VF sensitivities obtained from the two methods globally and sectorally on each OCT device. Values from the three devices were compared using ANOVA. A P value < 0.05 was considered statistically significant.

Table 1. Study Participants' Demographic and Clinical Characteristics

	Cirrus			Spectralis			RTVue		
	Normal	Glaucoma	*P*	Normal	Glaucoma	*P*	Normal	Glaucoma	*P*
Age, y	66.9 ± 17.9	65.4 ± 14.7	0.099	64.9 ± 7.0	65.4 ± 14.7	0.099	64.8 ± 10.7	65.4 ± 14.7	0.55
Visual field MD, dB	0.2 ± 1.1	−18.7 ± 8.2	<0.001	−0.06 ± 0.9	−18.7 ± 8.2	<0.001	−0.04 ± 1.0	−18.7 ± 8.2	<0.001
Total deviation loss, dB									
Global	0.3 ± 0.9	−16.9 ± 8.1	<0.001	0.04 ± 1.1	−16.9 ± 8.1	<0.001	0.07 ± 1.0	−16.9 ± 8.1	<0.001
Superior field	0.2 ± 1.3	−19.2 ± 9.9	<0.001	0.05 ± 1.2	−19.2 ± 9.9	<0.001	0.03 ± 1.3	−19.2 ± 9.9	<0.001
Inferior field	0.2 ± 1.1	−19.8 ± 9.7	<0.001	−0.08 ± 1.0	−19.8 ± 9.7	<0.001	−0.09 ± 1.1	−19.8 ± 9.7	<0.001
RNFL thickness, μm									
Global	93.7 ± 9.7	58.8 ± 7.2	<0.001	100.9 ± 8.9	51.3 ± 12.9	<0.001	99.4 ± 9.2	67.0 ± 10.4	<0.001
Superior quadrant	119.4 ± 17.3	66.7 ± 11.5	<0.001	119.4 ± 14.2	58.9 ± 17.7	<0.001	122.2 ± 14.2	79.5 ± 14.5	<0.001
Inferior quadrant	122.2 ± 16.9	63.0 ± 13.7	<0.001	134.0 ± 17.7	60.2 ± 21.5	<0.001	122.9 ± 13.9	80.0 ± 17.0	<0.001

SD, standard deviation.

RNFL Dynamic Range Determination

The dynamic range of global and sectoral RNFL was determined for each OCT device by subtracting the average residual layer thickness of glaucoma patients from the average RNFL thickness of normal subjects. For comparison purposes, the dynamic range was calculated using the BCP, SLRCP, post-BCP, and post-SLRCP residuals. Knowing the test–retest variability (TRTV) of RNFL thickness measured with OCT, it is possible to determine for each device the average number of steps between normal RNFL thickness and the RNFL floor. This information is important to know because the greater the number of steps, the more opportunities there are to detect a significant change and the longer a glaucomatous patient can be followed until the RNFL reaches the floor either globally or for a given RNFL sector. The number of steps was determined by dividing the RNFL dynamic range by the tolerance limit of intervisit TRTV in glaucoma patients. In this study, we used tolerance limits of TRTV of 3.9 μm for Cirrus HD-OCT,[18] 4.95 μm for Spectralis,[19] and 4.3 μm for RTVue.[20]

Results

Participant General Characteristics

As shown in Table 1, the patients ($n = 58$, mean age 65.4 ± 14.7 years, visual field mean deviation [VFMD] −18.7 ± 8.2 dB) included 15 with moderate and 43 with severe glaucoma. The normal subjects were distributed as follows: 60 in the Spectralis group (mean age 64.5 ± 10.6 years, VFMD −0.06 ± 0.9 dB), 55 in the RTVue group (mean age 64.8 ± 10.7 years, VFMD −0.04 ± 1.03 dB), and 60 in the Cirrus group (mean age 66.9 ± 17.9 years, VFMD 0.24 ± 1.1 dB). The patients had a significantly worse VFMD and relative VF sensitivities and thinner RNFL parameters than the controls (all $P < 0.001$), but the two groups were comparable in age ($P > 0.05$). All RNFL parameters and relative VF sensitivities were thinner in glaucoma patients compared to normal subjects (all $P < 0.001$).

RNFL Floor

The results of the BCP and SLR analyses are shown in Table 2. Estimates for global residual layer from the BCP method, which indicates the thickness of the residual layer when the RNFL stops thinning, were 57.0 ± 1.3 μm on Cirrus, 49.2 ± 1.6 μm on Spectralis, and 64.7 ± 1.4 μm on RTVue (Table 2; Fig. 1, top row). The residual layers of the superior and inferior quadrants were thicker than the global residual thickness on all three devices. The global change point estimated from the BCP analysis was similar between devices (−22.2 ± 6.4 dB on Cirrus, −25.3 ± 4.8 dB on Spectralis, and −24.6 ± 5.2 dB on RTVue). The SLR method estimated the global change point and corresponding RNFL thickness, respectively, at −10.4 dB and

Table 2. Bayesian Change Point and Simple Linear Regression Change Point Estimates and Corresponding Retinal Nerve Fiber Layer (RNFL) Floor

	Bayesian Change Point		Simple Linear Regression	
	RNFL Floor, μm	VF Sensitivity, dB	RNFL Floor, μm	VF Sensitivity, dB
Cirrus				
Global	57.0 ± 1.3 (54.5; 59.6)	−22.2 ± 6.4 (−32.4; −10.6)	57.3 ± 1.2 (54.9; 59.7)	−10.4 ± 3.6 (−17.5; −3.3)
Superior quadrant	65.0 ± 2.4 (60.4; 69.7)	−22.2 ± 6.5 (−32.3; −9.6)	64.9 ± 2.4 (60.2; 69.6)	−13.9 ± 4.9 (−23.5; −4.3)
Inferior quadrant	61.2 ± 2.3 (56.8; 65.8)	−21.1 ± 7.7 (−32.9; −7.7)	65.5 ± 2.2 (61.2; 69.8)	−12.6 ± 4.1 (−20.6; −4.6)
Spectralis				
Global	49.2 ± 1.6 (46.0; 52.3)	−25.3 ± 4.8 (−32.6; −15.7)	48.3 ± 1.5 (45.4; 51.2)	−14.0 ± 4.7 (−23.2; −4.8)
Superior quadrant	57.8 ± 2.6 (52.6; 62.9)	−23.7 ± 5.7 (−32.4; −12.4)	58.3 ± 2.7 (53.0; 63.6)	−13.2 ± 4.0 (−21.0; −5.4)
Inferior quadrant	60.1 ± 2.9 (54.5; 66.0)	−23.7 ± 6.1 (−33.1; −11.5)	62.9 ± 2.6 (57.8; 68.0)	−13.4 ± 4.6 (−22.4; −4.4)
RTVue				
Global	64.7 ± 1.4 (62.1; 67.4)	−24.6 ± 5.2 (−32.5; −14.4)	63.9 ± 1.3 (61.4; 66.5)	−14.4 ± 4.7 (−23.6; −5.2)
Superior quadrant	76.7 ± 2.2 (72.3; 80.9)	−22.6 ± 6.3 (−32.3; −10.2)	78.9 ± 2.3 (74.4; 83.4)	−11.3 ± 5.9 (−22.9; 0.3)
Inferior quadrant	78.0 ± 2.4 (73.5; 82.8)	−19.3 ± 8.4 (−32.8; −6.0)	84.4 ± 1.9 (80.7; 88.1)	−11.7 ± 5.4 (−22.3; −1.1)

Values in parentheses indicate lower and upper 95% confidence intervals.

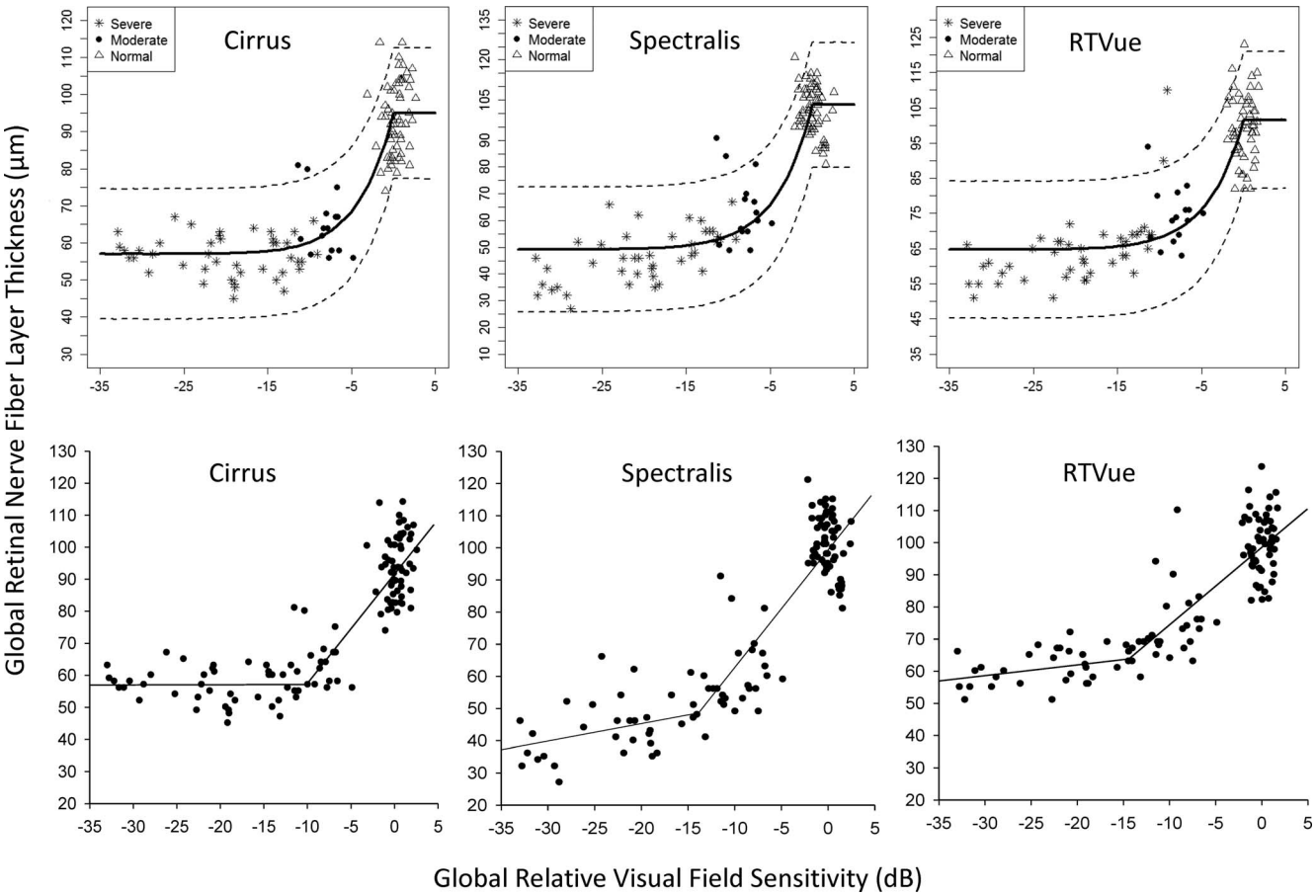

Figure 1. Bayesian change point plots (*top row*) and simple linear regression plots (*bottom row*) of the structure–function relationship of average RNFL thickness measured with Cirrus (**A**), Spectralis (**B**), and RTVue (**C**) with SAP average relative VF sensitivity. On simple linear regression plots, the meeting point between the two regression lines provides the coordinates of the amount of VF loss and corresponding residual layer thickness.

57.3 μm for Cirrus, −14.0 dB and 49.2 μm for Spectralis, and −14.4 dB and 64.7 μm for RTVue (Fig. 1, bottom row). The RNFL in the superior and inferior quadrants on the three devices stopped thinning at relative VF sensitivities between −19.3 dB and −23.7 dB after reaching the floor earlier at relative VF sensitivities ranging between −11.3 dB and −14.4 dB. Residual layer thickness estimates by both methods from RTVue tended to be thicker than those from Cirrus and Spectralis.

The global post-BCP residual layer was similar for Cirrus and RTVue (57.6 ± 5.0 vs. 58.4 ± 4.6 μm, $P = 0.95$), but significantly thicker than that measured with Spectralis (48.0 ± 7.7 μm, $P < 0.001$) (Table 3). Post-BCP residuals in the superior and inferior quadrants did not differ on each device, but significantly differed among devices (all $P < 0.01$). Similarly, the post-SLRCP residuals for global and superior and inferior quadrants were thicker than residuals in the nasal

Table 3. Post–Bayesian Change Point (BCP) and Post–Simple Linear Regression (SLRCP) Residual Layer Thickness and Corresponding Relative Visual Field Sensitivities

	Post-BCP Residual, μm	Post-SLRCP Residual, μm	*P*	Post-BCP VF Loss, dB	Post-SLRCP VF Loss, dB	*P*
Cirrus						
Global	57.6 ± 5.0 (54.8; 60.5)	57.1 ± 6.5 (55.2; 59.1)	0.79	−28.4 ± 3.7 (−30.5; −26.2)	−20.0 ± 7.0 (−22.2; −17.9)	<0.01
Superior quadrant	63.5 ± 8.4 (60.2; 66.8)	63.3 ± 8.4 (60.4; 66.1)	0.91	−28.3 ± 3.4 (−29.6; −27.0)	−25.7 ± 5.3 (−27.7; −24.3)	0.03
Inferior quadrant	59.8 ± 12.9 (54.7; 64.9)	61.8 ± 14.0 (57.3; 66.4)	0.55	−29.2 ± 3.9 (−30.7; −27.6)	−25.1 ± 7.0 (−27.4; −22.9)	<0.01
Spectralis						
Global	48.0 ± 7.7 (42.5; 53.5)	44.1 ± 9.3 (41.2; 47.6)	0.51	−30.3 ± 2.2 (−31.9; −28.7)	−23.0 ± 5.8 (−24.6; −20.3)	<0.01
Superior quadrant	53.2 ± 16.4 (45.9; 60.4)	53.4 ± 14.3 (48.4; 58.0)	0.95	−29.1 ± 2.9 (−30.4; −27.9)	−25.7 ± 5.3 (−27.5; −24.0)	<0.01
Inferior quadrant	53.8 ± 23.4 (43.7; 63.9)	56.8 ± 21.5 (49.7; 64.0)	0.88	−30.3 ± 2.9 (−31.6; −29.1)	−25.8 ± 6.6 (−28.0; −23.6)	<0.01
RTVue						
Global	58.4 ± 4.6 (55.3; 61.4)	61.2 ± 5.6 (58.2; 63.5)	0.14	−29.8 ± 2.6 (−31.6; −28.0)	−23.3 ± 5.7 (−28.0; −23.8)	<0.01
Superior quadrant	74.8 ± 9.0 (71.3; 78.4)	75.6 ± 9.6 (71.9; 78.6)	0.74	−28.3 ± 3.4 (−29.6; −27.0)	−24.3 ± 6.4 (−29.2; −26.4)	<0.01
Inferior quadrant	76.0 ± 17.5 (69.2; 82.7)	78.9 ± 18.6 (69.6; 81.9)	0.52	−28.8 ± 4.2 (−30.5; −27.2)	−24.5 ± 7.4 (−25.7; −22.1)	<0.01

Values in parentheses indicate lower and upper 95% confidence intervals.

Table 4. RNFL Dynamic Range and Number of Steps From Normal RNFL to the Floor

	Dynamic Range, μm		Number of Steps	
	SLRCP	Post-SLRCP	SLRCP	Post-SLRCP
Cirrus				
Global	35.4	36.6	9.0	9.4
Superior quadrant	54.5	56.1	7.8	8.0
Inferior quadrant	56.7	60.4	8.6	9.2
Spectralis				
Global	52.6	56.8	10.6	11.5
Superior quadrant	61.1	66.0	7.6	8.3
Inferior quadrant	71.1	76.9	9.2	9.9
RTVue				
Global	35.5	38.2	8.3	8.9
Superior quadrant	43.3	46.6	4.5	4.9
Inferior quadrant	38.5	44.0	4.8	5.4

and temporal quadrants on all three devices (Table 3). No significant differences were found between post-BCP and post-SLRCP residual layer thicknesses on any of the devices (all $P > 0.05$). In contrast, corresponding post-BCP relative VF sensitivities (range, −29.2 to −28.3 dB for Cirrus, −30.3 to −29.1 dB for Spectralis, and −29.8 to −28.3 dB for RTVue) were significantly lower than post-SLRCP sensitivities (range, −25.7 to −20.0 dB on Cirrus, −25.8 to −23.0 dB for Spectralis, and −24.5 to −23.3 dB for RTVue) (all $P < 0.05$).

RNFL Dynamic Range and Number of Steps to RNFL Floor

The dynamic range for global and sectoral RNFL on the three OCT devices, estimated using both the residual layer thickness obtained at the time RNFL thinning first reaches the floor and the average of all RNFL thicknesses with VF sensitivity equal to or worse than the SLR change, is listed in Table 4. The global RNFL dynamic range on Spectralis (52.6 μm) was wider than on Cirrus (35.4 μm) and RTVue (35.5 μm). Spectralis also showed wider dynamic ranges for the superior and inferior quadrant RNFL compared to Cirrus and RTVue, as did Cirrus relative to RTVue. The number of steps from normal global RNFL thickness to the floor was 9.0 on Cirrus, 10.6 on Spectralis, and 8.3 on RTVue (Table 4; Fig. 2). Cirrus and Spectralis also had a similar number of steps for superior and inferior quadrant RNFL, which were greater than the step counts on RTVue.

Discussion

Regardless of the primary risk factor, there is a general consensus that glaucoma is a slowly progressive neurodegenerative disease associated with death of retinal ganglion cells and degeneration of their axons. Structurally, this is manifested, among other things, by progressive RNFL thinning until the floor is reached if the disease is left untreated or not adequately treated. Although past studies have described the course of RNFL thinning prior to reaching the floor,[6,12,13,21] one unaddressed question has been whether the floor corresponds to the end of the thinning process. With the availability of several SDOCT platforms currently used in the clinical setting, it also has largely remained unclear how these platforms compare to each other with regard to RNFL floor and dynamic range. In this study, we used two statistical methods to estimate the amounts of relative VF sensitivity at which RNFL thinning reaches the floor and at which RNFL thinning subsequently stops (change points), the dynamic range of RNFL thickness, and the number of steps from normal RNFL to RNFL floor. The values were compared among three SDOCT platforms.

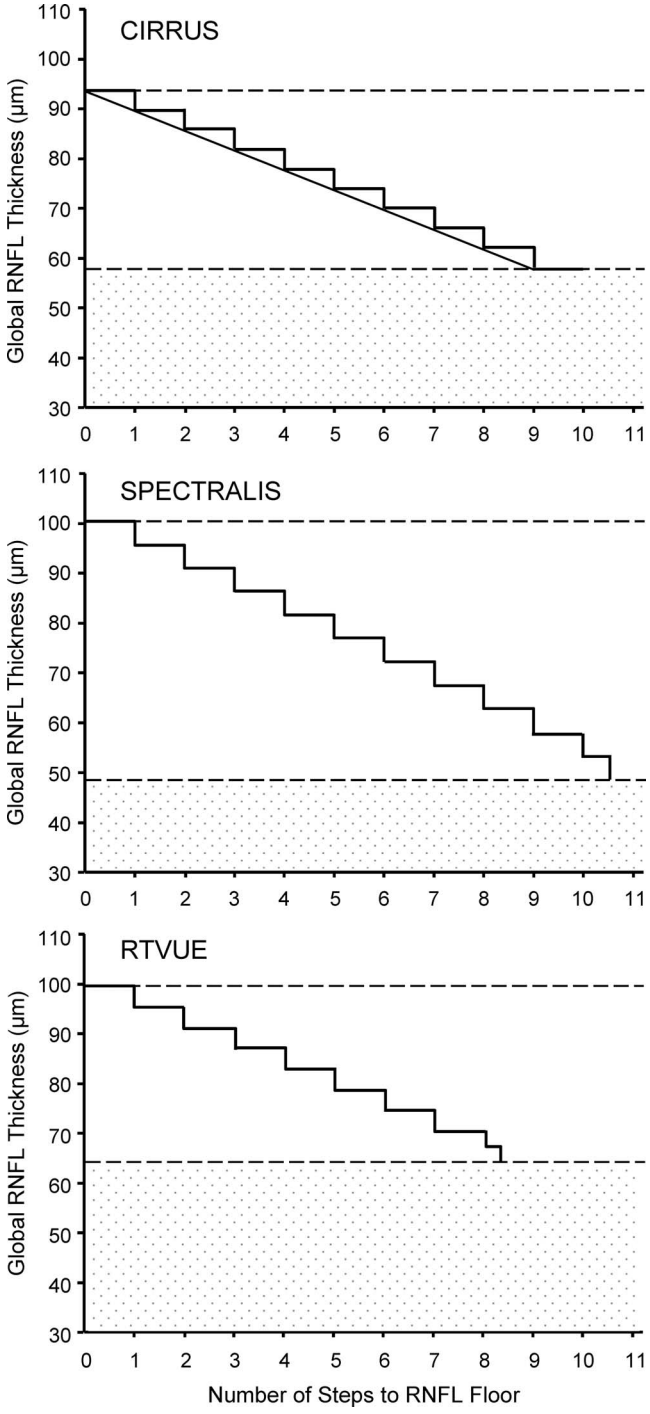

Figure 2. Staircase representation of the number of steps from normal average RNFL thickness to average RNFL floor on Cirrus, Spectralis, and RTVue. The *upper and lower dashed lines* indicate the values of normal RNFL thickness and floor, respectively; the *space* between them is the dynamic range. The *height of the steps* on each plot represents the TRTV. The *patterned area* represents the residual layer thickness. The *straight line* connecting the stairs in the Cirrus plot indicates that RNFL actually thins continuously rather than in steps.

Our results indicate that (1) RNFL thinning reaches the floor at relative VF sensitivity greater than when the thinning ends, without significant differences in their corresponding residual layer thicknesses; (2) the measured thicknesses at the time RNFL reaches the floor and when the thinning process ends differed among the three OCT platforms, and (3) the dynamic range of RNFL also varied among the devices, whereas the number of steps from normal RNFL to RNFL floor did not vary much among them. These findings have significant clinical implications for the use of OCT and VF to monitor glaucoma patients.

The reason RNFL measurements do not go all the way to zero in glaucoma has been well documented histologically; its architectural support, made of the retinal glial cells (Müller cells, astroglia, microglia) and vessels, does not degenerate concurrently with the retinal ganglion cell axons. Quigley and Addicks[22] showed in primates that RNFL damage with total loss of axons following experimental lesions to the optic nerve leaves a mixture of capillaries, astrocytes, and Müller cells, with significant variations in the ratio of axons to supportive tissue at different locations. In addition, it has been shown that, as a response to progressive glaucomatous axonal loss, the RNFL layer may undergo remodeling, including glial cell proliferation.[23,24]

Linear models of the relationship between cross-sectional SDOCT RNFL and SAP data have indicated that RNFL layer thickness measurements reach the lower end of their dynamic range while there is still remaining function.[13,25] This is corroborated by our findings that average RNFL thickness measured with Cirrus, Spectralis, and RTVue reached the floor at relative VF sensitivities of −10.4, −14.0, and −14.4 dB, respectively. In other words, since the relative VF sensitivity ranges between 0 dB (no loss corresponding to low-contrast stimulus, i.e., in healthy subjects) and approximately −35 dB (complete loss corresponding to high-contrast stimulus), 70.3%, 60.3%, and 58.9% of global function still remained at the time RNFL reached the measured floor. The average residual layer thicknesses were 61.2% (Cirrus), 47.9% (Spectralis), and 64.3% (RTVue) of healthy subject values. The clinical relevance of this finding is the potential for monitoring patients using functional tests after structural measures have reached the floor. Kanamori et al.[26] studied the relationship of VF sensitivity with RNFL thickness measured with Cirrus, RTVue, and three-dimensional OCT 2000 (Topcon, Inc., Tokyo, Japan) using the Hood and Kardon linear model. They reported average residual layer thicknesses of 60.6, 69.7, and 64.7 μm, respectively, which represented 64.6%, 68.3%, and 61.5% of RNFL thickness of the controls. They did not mention the corresponding sensitivity losses. As has been shown previously by others,[7,27–30] our results also suggest that the structure–function relationship in glaucoma varies over time so that structural measures are more sensitive in early stages, whereas functional measures provide more information in advanced disease. Rather than VF being spared in early stages of the disease, this differential behavior between structural and functional measures in glaucoma may be due to SAP inability to detect small functional loss, as a result of the redundancy of the visual system and the overlap of receptive fields. Interestingly, other functional tests such as short-wavelength automated perimetry, flicker perimetry, high-pass resolution perimetry, frequency doubling technology perimetry, and pattern electroretinogram have demonstrated the ability to detect glaucomatous functional damage earlier than achromatic perimetry.[31–37]

In the present study, the residual layer thicknesses in the superior and inferior quadrants were, respectively, 54.4% and 53.6% (Cirrus), 48.8% and 46.9% (Spectralis), and 64.6% and 68.7% (RTVue) relative to controls, indicating thicker residuals on RTVue compared to Cirrus and Spectralis. In a recent retrospective study, we also reported that residual thicknesses on Spectralis were 47.5% and 45.4% relative to controls in the superior and inferior quadrants, respectively, compared to 70.7% and 62.7% for RTVue.[15] An analysis of RTVue RNFL data from the Diagnostic Innovation in Glaucoma Study (DIGS) and African Descent and Glaucoma Evaluation Study (ADAGES) using the Hood and Kardon linear model found a residual of 83.3 μm or 60% of normal RNFL thickness in the inferotemporal sector and 80.7 μm or 61% of normal RNFL thickness.[13] A subsequent study by the same investigators using Cirrus RNFL data reported residual thicknesses of 61.2 μm (46% of normal RNFL) in the inferotemporal and 60.4 μm (49% of normal RNFL) in the superotemporal region.[25] In contrast, application of the same analytical model to Spectralis and SAP data from 27 healthy eyes and 68 eyes with early to advanced glaucoma estimated a greater residual layer thickness in the inferotemporal (54.3 μm) than in the superotemporal sector (80.8 μm).[38] While the interdevice difference in absolute residual layer thickness we found has to be ascribed mostly to the difference in segmentation algorithms, the discrepancies across studies using the same device is likely influenced by the anatomical differences in study populations, the use of different structure–function relationship mapping schemes, and statistical methods.

We recently reported on estimates of the amount of relative VF sensitivity and corresponding residual layer thickness at the time RNFL measured with Spectralis and RTVue stops thinning in glaucoma.[15] That study, performed retrospectively and in different subjects for each device, as well as the current study, performed prospectively and using the same glaucoma subjects across all the devices, show that RNFL thinning stops in the late stage of the disease. Thus, RNFL thinning progresses after reaching the floor, but the slope is not significant as demonstrated by the lack of difference between residual layer thicknesses at the time the RNFL reaches the floor and when it stops thinning. Likewise, Hood et al.[11] found a weak and nonsignificant thinning of the residual thickness over time from the last episode of anterior ischemic optic neuropathy. Putting this information in the context of the dynamic range of structural and functional measures, our findings confirm the observation that RNFL thickness has a shorter dynamic range than VF measures as determined by SAP. Thus, the short dynamic range of RNFL is a limiting factor for exploring and describing the structure–function relationship in glaucoma once relative VF sensitivity becomes lower than −10 dB and the RNFL thickness is approximately 50 to 55 μm for Cirrus and Spectralis and 65 μm for RTVue. Unlike VF assessment, the dynamic range of RNFL thickness cannot be expanded once it reaches the floor. As for VF, the Humphrey Field Analyzer 24-2 program with a size III stimulus is the most commonly used testing mode. The mean deviation (MD) or VF index (VFI) can help stage the disease, with the difference between the two being that other causes than glaucoma may reduce the MD. In contrast, the VFI measures visual function loss caused by glaucomatous damage only, and its dynamic range varies between 100% (full field) and 0% (complete field loss). When VF seems to be completely lost through the 24-2 test pattern and size III stimulus, the dynamic range of the VF can be increased by switching to a size V stimulus, allowing function to still be monitored after the dynamic range of the RNFL has reached the lower end. With further field loss, more dynamic range expansion is possible using the 10-2 test with a size V stimulus and 2° grid points spacing, which allows crowding of a greater number of testing points in a small area.[39]

The concept of numbering steps from normal RNFL to the RNFL floor is a useful clinical parameter that is complementary to the RNFL dynamic range. It may represent another objective way of monitoring and staging the disease, as it indicates where the patient stands on the RNFL thickness "stairway" from

Investigative Ophthalmology & Visual Science

normal RNFL to its floor. We have found that despite some differences in dynamic range, the three OCT platforms were in fact comparable with regard to the number of steps from normal RNFL to the floor. The number of steps for average RNFL thickness was 9.0 on Cirrus, 10.6 on Spectralis, and 8.3 on RTVue. These figures are based on current TRTV for each device. It remains unclear whether these numbers are expected to increase as a result of further improvement in the future with regard to segmentation algorithm, increase in axial resolution, and decrease in TRTV. It should be noted that a caveat to this concept of steps is that in the real world the RNFL does not thin in a series of steps but rather in a continuous manner, as illustrated by the straight line connecting the steps in Figure 2 (top). It could also be argued that because the number of steps to the RNFL floor is a function of the RNFL TRTV, which in turn may considerably differ across studies, the most appropriate design would have been to measure RNFL thickness in the same group of subjects with the three OCT devices and to calculate the RNFL TRTVs. While future studies are needed using this design, it is likely that the TRTVs may remain different because the three devices are known to generate different RNFL thickness values.

Prior studies based on the Hood and Kardon model have estimated the residual layer thickness by averaging the RNFL thicknesses of all subjects with relative VF sensitivity worse than −10 dB.[6,12,13,21,25,38] This cutoff value was estimated to be the asymptotic point and was determined by simple visual inspection of the curve of the relationship between RNFL and SAP. While the SLR method used herein roughly agreed with Hood and Kardon's predictions with regard to the asymptotic point, it also showed that the asymptotic point may be variable, which confirms our recent findings.[15] Interestingly, the predicted residual thicknesses by the SLR method were comparable to thicknesses obtained by averaging all residual layers in subjects with relative VF sensitivities equal to or worse than the asymptotic points. The corollary to this finding is that the SLR method was accurate in predicting the value of the residual layer thickness, and it represents a reliable alternative to the averaging method.

Some important aspects should be considered when interpreting our findings or attempting to apply them to individual patients or other population groups. First, one should keep in mind the cross-sectional nature of the data, so that the results may differ from those obtained if longitudinal data are used. Glaucoma is a slowly progressing disease, and thus determining longitudinally when RNFL thinning reaches the floor or when RNFL stops completely thinning requires decades of follow-up. Because this has not been possible so far, studies determining the trend of the structure–function relationship in glaucoma over time have, as in the present study, alternatively relied on mathematical or statistical models using cross-sectional data across all severity stages of the disease.[13,21,25,29] Interestingly, RNFL thickness values derived from the BCP model were lower, although not significantly, than those from the SLR model, suggesting that reaching the floor may not correspond to the end of the thinning process. Second, our results may have been influenced by the effect of age on RNFL thinning,[40] residual thickness,[11] and VF sensitivity reduction.[41] In order to minimize these effects, we used VF total deviation values, which are age corrected, and we age matched normal and glaucoma subjects. Third, the large variability in the number of retinal ganglion cell axons and thus in RNFL thickness across the normal population implies that the results may differ from one study population to another. Fourth, a compromise is yet to be found on which estimation or analytical model better characterizes the correlation between structural and functional loss in glaucoma; interestingly the models used in the present study generated results that are comparable to those of previous studies despite differing statistical methods. Fifth, multiple SDOCT devices by different manufacturers are currently available for clinical use. The lack of standardization with regard to optical properties, axial resolution, scanning speed, light source characteristics, segmentation algorithm, and image processing capabilities has resulted in systematic measurement differences among different OCT platforms.[42,43] From a practical standpoint, such differences prevent longitudinal monitoring of patients' OCTs from different manufacturers; they also prevent the comparison of OCT data during multicenter clinical trials if participating centers use different OCT platforms. One way of circumventing this challenge is to normalize OCT data from different OCTs. Therefore, application of measurement normalization to our data could have resulted in fewer discrepancies between devices, allowing generalization of our findings across instruments. Indeed, earlier studies have reported reduction in RNFL thickness measurements between two different SD-OCT devices following signal normalization.[44–46]

In conclusion, the number of steps to the average RNFL floor is similar among the three devices despite differences in residual layer thickness, RNFL dynamic range, and the amount of relative VF sensitivity at which average RNFL reaches the floor. The RNFL reaches the floor while more than 50% of visual function remains.

Acknowledgments

The authors thank the investigators of the National Eye Institute–sponsored Diagnostic Innovations in Glaucoma Study (NEI R01EY011008, R01EY021818, P30EY022589) conducted at the University of California, San Diego (UCSD), California, United States, for providing part of the data used in this study.

Presented at the annual meeting of the Association for Research in Vision and Ophthalmology, Denver, Colorado, United States, May 3–7, 2015.

Supported by Research to Prevent Blindness (RPB), New York, New York, United States.

Disclosure: **J.-C. Mwanza**, None; **H.Y. Kim**, None; **D.L. Budenz**, None; **J.L. Warren**, None; **M. Margolis**, None; **S.D. Lawrence**, None; **P.D. Jani**, None; **G.S. Thompson**, None; **R.K. Lee**, None

References

1. Garway-Heath DF, Holder GE, Fitzke FW, Hitchings RA. Relationship between electrophysiological, psychophysical, and anatomical measurements in glaucoma. *Invest Ophthalmol Vis Sci*. 2002;43:2213–2220.
2. Schlottmann PG, De Cilla S, Greenfield DS, Caprioli J, Garway-Heath DF. Relationship between visual field sensitivity and retinal nerve fiber layer thickness as measured by scanning laser polarimetry. *Invest Ophthalmol Vis Sci*. 2004;45:1823–1829.
3. Leung CK, Chong KK, Chan WM, et al. Comparative study of retinal nerve fiber layer measurement by StratusOCT and GDx VCC, II: structure/function regression analysis in glaucoma. *Invest Ophthalmol Vis Sci*. 2005;46:3702–3711.
4. Harwerth RS, Quigley HA. Visual field defects and retinal ganglion cell losses in patients with glaucoma. *Arch Ophthalmol*. 2006;124:853–859.
5. Harwerth RS, Wheat JL, Fredette MJ, Anderson DR. Linking structure and function in glaucoma. *Prog Retin Eye Res*. 2010; 29:249–271.
6. Hood DC, Kardon RH. A framework for comparing structural and functional measures of glaucomatous damage. *Prog Retin Eye Res*. 2007;26:688–710.

7. Wollstein G, Schuman JS, Price LL, et al. Optical coherence tomography longitudinal evaluation of retinal nerve fiber layer thickness in glaucoma. *Arch Ophthalmol*. 2005;123:464–470.
8. Swanson WH, Felius J, Pan F. Perimetric defects and ganglion cell damage: interpreting linear relations using a two-stage neural model. *Invest Ophthalmol Vis Sci*. 2004;45:466–472.
9. Blumenthal EZ, Horani A, Sasikumar R, Garudadri C, Udaykumar A, Thomas R. Correlating structure with function in end-stage glaucoma. *Ophthalmic Surg Lasers Imaging*. 2006;37:218–223.
10. Sihota R, Sony P, Gupta V, Dada T, Singh R. Diagnostic capability of optical coherence tomography in evaluating the degree of glaucomatous retinal nerve fiber damage. *Invest Ophthalmol Vis Sci*. 2006;47:2006–2010.
11. Hood DC, Anderson S, Rouleau J, et al. Retinal nerve fiber structure versus visual field function in patients with ischemic optic neuropathy. A test of a linear model. *Ophthalmology*. 2008;115:904–910.
12. Kim SH, Jeoung JW, Park KH, Kim TW, Kim DM. Correlation between retinal nerve fiber layer thickness and visual field sensitivity: diffuse atrophy imaging study. *Ophthalmic Surg Lasers Imaging*. 2012;43:S75–S82.
13. Rao HL, Zangwill LM, Weinreb RN, Leite MT, Sample PA, Medeiros FA. Structure-function relationship in glaucoma using spectral-domain optical coherence tomography. *Arch Ophthalmol*. 2011;129:864–871.
14. Hodapp E, Parrish RKI, Anderson DR. *Clinical Decisions in Glaucoma*. St. Louis: Mosby-Year Book; 1993:52–61.
15. Mwanza JC, Budenz DL, Warren JL, et al. Retinal nerve fibre layer thickness floor and corresponding functional loss in glaucoma. *Br J Ophthalmol*. 2015;99:732–737.
16. Carlin BP, Gelfand AE, Smith AFM. Hierarchical Bayesian analysis of changepoint problems. *J R Stat Soc Ser C Appl Stat*. 1992;41:389–405.
17. Wollstein G, Kagemann L, Bilonick RA, et al. Retinal nerve fibre layer and visual function loss in glaucoma: the tipping point. *Br J Ophthalmol*. 2012;96:47–52.
18. Mwanza JC, Chang RT, Budenz DL, et al. Reproducibility of peripapillary retinal nerve fiber layer thickness and optic nerve head parameters measured with cirrus HD-OCT in glaucomatous eyes. *Invest Ophthalmol Vis Sci*. 2010;51:5724–5730.
19. Tan BB, Natividad M, Chua KC, Yip LW. Comparison of retinal nerve fiber layer measurement between 2 spectral domain OCT instruments. *J Glaucoma*. 2012;21:266–273.
20. Garas A, Vargha P, Hollo G. Reproducibility of retinal nerve fiber layer and macular thickness measurement with the RTVue-100 optical coherence tomograph. *Ophthalmology*. 2010;117:738–746.
21. Hood DC, Anderson SC, Wall M, Kardon RH. Structure versus function in glaucoma: an application of a linear model. *Invest Ophthalmol Vis Sci*. 2007;48:3662–3668.
22. Quigley HA, Addicks EM. Quantitative studies of retinal nerve fiber layer defects. *Arch Ophthalmol*. 1982;100:807–814.
23. Varela HJ, Hernandez MR. Astrocyte responses in human optic nerve head with primary open-angle glaucoma. *J Glaucoma*. 1997;6:303–313.
24. Wang L, Cioffi GA, Cull G, Dong J, Fortune B. Immunohistologic evidence for retinal glial cell changes in human glaucoma. *Invest Ophthalmol Vis Sci*. 2002;43:1088–1094.
25. Leite MT, Zangwill LM, Weinreb RN, Rao HL, Alencar LM, Medeiros FA. Structure-function relationships using the Cirrus spectral domain optical coherence tomograph and standard automated perimetry. *J Glaucoma*. 2012;21:49–54.
26. Kanamori A, Nakamura M, Tomioka M, Kawaka Y, Yamada Y, Negi A. Structure-function relationship among three types of spectral-domain optical coherent tomography instruments in measuring parapapillary retinal nerve fibre layer thickness. *Acta Ophthalmol*. 2013;91:e196–e202.
27. Fayers T, Strouthidis NG, Garway-Heath DF. Monitoring glaucomatous progression using a novel Heidelberg Retina Tomograph event analysis. *Ophthalmology*. 2007;114:1973–1980.
28. Leung CK, Cheung CY, Weinreb RN, et al. Evaluation of retinal nerve fiber layer progression in glaucoma: a study on optical coherence tomography guided progression analysis. *Invest Ophthalmol Vis Sci*. 2010;51:217–222.
29. Medeiros FA, Lisboa R, Weinreb RN, Liebmann JM, Girkin C, Zangwill LM. Retinal ganglion cell count estimates associated with early development of visual field defects in glaucoma. *Ophthalmology*. 2013;120:736–744.
30. Strouthidis NG, Scott A, Peter NM, Garway-Heath DF. Optic disc and visual field progression in ocular hypertensive subjects: detection rates, specificity, and agreement. *Invest Ophthalmol Vis Sci*. 2006;47:2904–2910.
31. Banitt MR, Ventura LM, Feuer WJ, et al. Progressive loss of retinal ganglion cell function precedes structural loss by several years in glaucoma suspects. *Invest Ophthalmol Vis Sci*. 2013;54:2346–2352.
32. Brusini P, Busatto P. Frequency doubling perimetry in glaucoma early diagnosis. *Acta Ophthalmol Scand Suppl*. 1998;227:23–24.
33. Cello KE, Nelson-Quigg JM, Johnson CA. Frequency doubling technology perimetry for detection of glaucomatous visual field loss. *Am J Ophthalmol*. 2000;129:314–322.
34. Demirel S, Johnson CA. Incidence and prevalence of short wavelength automated perimetry deficits in ocular hypertensive patients. *Am J Ophthalmol*. 2001;131:709–715.
35. Johnson CA, Brandt JD, Khong AM, Adams AJ. Short-wavelength automated perimetry in low-, medium-, and high-risk ocular hypertensive eyes. Initial baseline results. *Arch Ophthalmol*. 1995;113:70–76.
36. Landers J, Goldberg I, Graham S. A comparison of short wavelength automated perimetry with frequency doubling perimetry for the early detection of visual field loss in ocular hypertension. *Clin Experiment Ophthalmol*. 2000;28:248–252.
37. Ventura LM, Sorokac N, De Los Santos R, Feuer WJ, Porciatti V. The relationship between retinal ganglion cell function and retinal nerve fiber thickness in early glaucoma. *Invest Ophthalmol Vis Sci*. 2006;47:3904–3911.
38. Pinto LM, Costa EF, Melo LA Jr, et al. Structure-function correlations in glaucoma using matrix and standard automated perimetry versus time-domain and spectral-domain OCT devices. *Invest Ophthalmol Vis Sci*. 2014;55:3074–3080.
39. Anders H, Patella VM, Bengtsson N. *The Field Analyzer Primer: Effective Perimetry*. 4th ed. Carl Zeiss Meditec, Inc.; 2012:32.
40. Budenz DL, Anderson DR, Varma R, et al. Determinants of normal retinal nerve fiber layer thickness measured by Stratus OCT. *Ophthalmology*. 2007;114:1046–1052.
41. Spry PG, Johnson CA. Senescent changes of the normal visual field: an age-old problem. *Optom Vis Sci*. 2001;78:436–441.
42. Buchser NM, Wollstein G, Ishikawa H, et al. Comparison of retinal nerve fiber layer thickness measurement bias and imprecision across three spectral-domain optical coherence tomography devices. *Invest Ophthalmol Vis Sci*. 2012;53:3742–3747.
43. Pierro L, Gagliardi M, Iuliano L, Ambrosi A, Bandello F. Retinal nerve fiber layer reproducibility using seven different OCT instruments. *Invest Ophthalmol Vis Sci*. 2012;53:5912–5920.
44. Chen CL, Ishikawa H, Wollstein G, et al. Individual A-scan signal normalization between two spectral domain optical coherence tomography devices. *Invest Ophthalmol Vis Sci*. 2013;54:3463–3471.
45. Chen CL, Ishikawa H, Wollstein G, et al. Signal normalization reduces systematic measurement differences between spectral-domain optical coherence tomography devices. *Invest Ophthalmol Vis Sci*. 2013;54:7317–7322.
46. Hu Z, Nittala MG, Sadda SR. Comparison of retinal nerve layer intensity profiles from different OCT devices. *Ophthalmic Surg Lasers Imaging Retina*. 2013;44:S5–S10.

Investigative Ophthalmology & Visual Science